CrystEngComm

ROYAL SOCIETY OF CHEMISTRY

PAPER

View Article Online
View Journal | View Issue

Cite this: *CrystEngComm*, 2024, **26**, 5039

Structural polymorphism and luminescence properties of zinc(II) and cobalt(II) MOFs with rigid and flexible ligands†

Pavel V. Burlak, Denis G. Samsonenko, Konstantin A. Kovalenko * and Vladimir P. Fedin *

Received 7th June 2024,
Accepted 23rd July 2024

DOI: 10.1039/d4ce00573b

rsc.li/crystengcomm

Here, we present a series of Zn(II) and Co(II) coordination polymers containing two types of ligands: sterically rigid terephthalate derivatives (bdc-NO_2^{2-} and bdc-Br^{2-}) and flexible bis(2-methylimidazolyl) propane (bmip). The combination of two types of ligands allowed us to obtain and characterize both single and mixed-metal compounds by single crystal and powder X-ray diffraction, FT-IR, and elemental analysis. These 4-fold interpenetrated frameworks have a diamond topology and do not reveal any structural transformations despite the presence of a flexible ligand. Luminescence spectra for all the Zn-containing compounds were recorded. All the compounds exhibit a strong dependence of emission maxima on excitation wavelength, which is characteristic of the bmip ligand and is enhanced in coordination polymers. Compound [Zn(bdc-Br)(bmip)] demonstrates bright luminescence with a high quantum yield of 39%. Mixed-metal Zn(II)/Co(II) compounds have redshifted luminescence in comparison to [Zn(bdc-NO_2)(bmip)] and compound [$Zn_{0.6}Co_{0.4}$(bdc-NO_2)(bmip)] is characterized by near white emission under 460 nm excitation.

1 Introduction

Metal–organic frameworks (MOFs) are one of the fastest developing classes of porous materials. MOFs possess high crystallinity, large specific surface areas and porosity, and huge structural diversity by combining a lot of types of metal nodes and organic linkers. All this makes MOFs promising materials for possible application in different fields: adsorption and separation,[1–5] luminescent materials,[6–14] catalysis[15–19] and other areas.[20–25]

The most well-known and stable MOFs are constructed based on rigid carboxylates and N-donor ligands.[26–30] Using rigid carboxylate ligands together with flexible N-donor ligands opens new opportunities in MOF design (Fig. 1).[31,32] Flexible N-donor ligands provide conformational lability to the synthesized framework leading to formation of more varieties of structures, while structurally rigid carboxylate ligands provide enough rigidity and negative charge for the creation of stable neutral frameworks.[33–38]

The bis(imidazolyl)alkane class of compounds is readily available due to the simplicity of the synthetic approach and can provide sufficient flexibility due to the alkyl spacers between the two imidazole rings. The use of ligands based

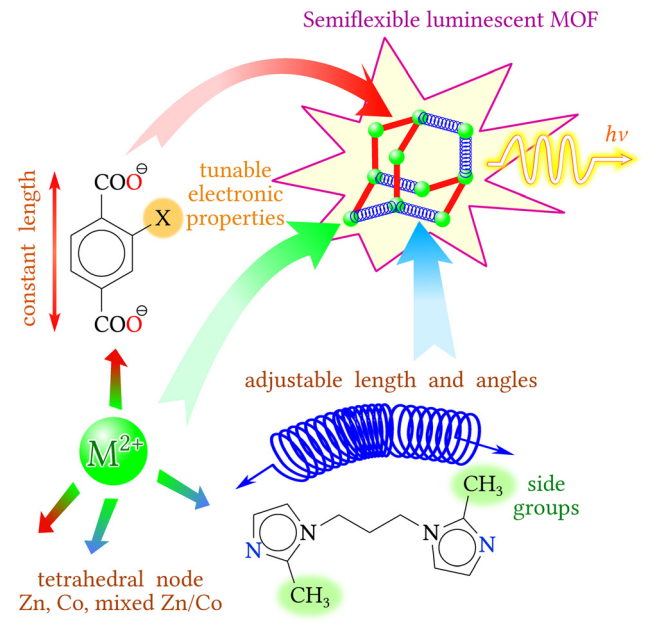

Fig. 1 Design idea of using flexible and rigid ligands with tetrahedrally coordinated metal nodes.

Nikolaev Institute of Inorganic Chemistry SB RAS, 3 Akad. Lavrentiev Av., 630090 Novosibirsk, Russian Federation. E-mail: k.a.kovalenko@niic.nsc.ru, cluster@niic.nsc.ru; Fax: +7 383 330 9489; Tel: +7 383 330 9490

† Electronic supplementary information (ESI) available: Methods, elemental analysis, structure visualization figures, luminescence emission spectra and chromaticity diagrams. CCDC 2358461–2358463. For ESI and crystallographic data in CIF or other electronic format see DOI: https://doi.org/10.1039/d4ce00573b

on unsubstituted imidazole often results in the formation of multiply interpenetrated frameworks.[39,40] The addition of a methyl substitute to the imidazolyl rings can lead to the formation of flexible porous MOFs.[41–45] Used in this work, 1,3-bis(2-methylimidazolyl)propane (bmip) is a readily available N-donor ditopic flexible organic ligand that at the same time does not have a too long aliphatic spacer and therefore exhibits good flexibility–rigidity balance. Having coordinated with metal centers, the flexible nature of the ligand allows it to bend and rotate, which often leads to structural diversity. On the other hand, the ability to change and adjust the structure allows the use of materials containing this type of ligand as sensors.[46–48]

The introduction of two types of metals into MOF nodes can lead to an improvement in the catalytic, electronic, and luminescence properties.[49–54] In addition, the proportions of metals in bimetallic MOFs can be easily adjusted and controlled, which, in turn, allows the fine tuning of the physicochemical properties of mixed-metal MOFs.[55–57]

Herein, we report the synthesis and determination the crystal structures of four new zinc(II) and cobalt(II) coordination polymers based simultaneously on structurally rigid bromo- or nitroterephthalate and structurally flexible 1,3-bis(2-methylimidazolyl)propane ligands. In addition, a series of mixed-metal phases $[Zn_xCo_{1-x}(bdc\text{-}NO_2)(bmip)]$ (x = 0.8, 0.6, 0.4) were also obtained and characterized.

2 Materials and syntheses

2.1 Materials

All chemicals and solvents were commercially available with purity not lower than "chemically pure" and used as received without further purification. The synthesis of 1,3-bis(2-methylimidazolyl)propane was carried out according to a procedure described elsewhere.[39,41,42]

The analysis of topologies was performed with **https://topcryst.com**.[58] The RCSR three-letter codes[59] were used to designate the network topologies. Those nets that are absent in the RCSR are designated with the TOPOS *NDn* nomenclature,[60] where *N* is a sequence of coordination numbers of all non-equivalent nodes of the net, *D* is the periodicity of the net (*D* = *M*, *C*, *L*, *T* for 0-, 1-, 2-, 3-periodic nets), and *n* is the ordinal number of the net in the set of all non-isomorphic nets with the given *ND* sequence. To calculate the underlying nets, we used algorithms,[60] the application of which for specific structures is discussed in the article.[61] The TTD collection[62] was used to determine the topological type of the crystal structure.

2.2 Syntheses of compounds

All syntheses were carried out using a similar procedure. Synthetic details, such as weight of metal salt and carboxylic acid, for each synthesis are given in Table 1. In general, metal salt (0.25 mmol in total), carboxylic acid (0.25 mmol), bmip (0.25 mmol, 51 mg), DMF (13.75 mL), and 10 mL of alcohol (MeOH or EtOH) were heated at 373 K for 1 day in a glass vial with a screw cap. The resulting crystals were separated by decantation, washed with ROH (3 × 5 mL) and dried in air. Yields (based on metal) are 40–60%.

For compounds **1** and **2** single crystals were obtained and their crystal structures were determined using single crystal X-ray analysis (see Table S1,† Fig. 2). Crystals of compound **3** were not good enough for single-crystal X-ray analysis; therefore only a model of the structure was determined. According to powder X-ray diffraction, compounds **4**, **5**, **6** and **7** are isostructural to **1** and **2**. The composition of the compounds obtained were established by CHN elemental analysis. ICP-AES analysis was used to determine the metal ratio in the mixed-metal Zn/Co compounds. Results of elemental analysis for all the compounds obtained are summarized in Table S2.†

IR spectra (KBr; ν, cm^{-1}) **1**: 3436 (w br), 3154 (m), 3129 (m), 2960 (m), 1627 (s), 1533 (m), 1487 (m), 1427 (m), 1352 (s), 1286 (m) 1250 (w), 1156 (w), 1095 (w), 1064 (w), 1006 (w), 948 (w), 921 (w), 875 (w), 839 (m), 824 (m), 778 (s), 752 (m), 691 (m), 672 (w), 585(w), 508 (m), 447 (w).

2: 3436 (w br), 3151 (m), 3127 (m), 2960 (m), 1627 (s), 1509 (m), 1473 (m), 1427 (w), 1342 (s), 1287 (w), 1158 (w), 1088 (w), 1033 (w), 1008 (w), 948 (w), 912 (w), 878 (w), 827 (m), 770 (s), 735 (m), 675 (m), 585 (w), 525 (m), 441 (w).

3: 3436 (w br), 3151 (m), 3127 (m), 2960 (m), 1627 (s), 1550 (m), 1473 (m), 1427 (m), 1378 (s), 1289 (m), 1158 (w), 1088 (w), 1035 (w), 1008 (w), 948 (w), 912 (w), 878 (w), 839 (m), 827 (m), 766 (s), 735 (m), 672 (w), 585 (w), 522 (m), 442 (w).

4: 3436 (w br), 3151 (m), 3127 (m), 2960 (m), 1627 (s), 1550 (m), 1473 (m), 1427 (m), 1342 (s), 1287 (m), 1158 (w), 1088 (w), 1033 (w), 1008 (w), 948 (w), 912 (w), 878 (w), 827 (m), 770 (s), 735 (m), 691 (m), 675 (w), 585 (w), 525 (m), 441 (w).

5–7: 3436 (w br), 3154 (m), 3129 (m), 2960 (m), 1627 (s), 1533 (m), 1487 (w), 1427 (w), 1352 (S), 1286–1288 (w), 1156–1151 (w), 1095–1096 (w), 1064 (w), 1005–1008 (w), 948 (w),

Table 1 Chemical formula of compounds obtained, weight of reagents used in syntheses and yields

No.	Formula	$Zn(NO_3)_2{\cdot}6H_2O$	$Co(NO_3)_2{\cdot}6H2O$	Carboxylic acid	ROH	Yield
1	$[Zn(bdc{-}NO_2)(bmip)]$	0.26 mmol, 77 mg	—	0.25 mmol, 53 mg	EtOH	55%, 65 mg
2	$[Co(bdc{-}NO_2)(bmip)]$	—	0.25 mmol, 73 mg	0.25 mmol, 53 mg	MeOH	55%, 65 mg
3	[Zn(bdc–Br)(bmip)]	0.26 mmol, 77 mg	—	0.25 mmol, 61 mg	EtOH	60%, 77 mg
4	[Co(bdc–Br)(bmip)]	—	0.25 mmol, 73 mg	0.25 mmol, 61 mg	MeOH	40%, 51 mg
5	$[Zn_{0.8}Co_{0.2}(bdc\text{-}NO_2)(bmip)]$	0.2 mmol, 62 mg	0.05 mmol, 15 mg	0.25 mmol, 53 mg	EtOH	50%, 60 mg
6	$[Zn_{0.6}Co_{0.4}(bdc\text{-}NO_2)(bmip)]$	0.15 mmol, 47 mg	0.1 mmol, 30 mg	0.25 mmol, 53 mg	EtOH	50%, 60 mg
7	$[Zn_{0.4}Co_{0.6}(bdc\text{-}NO_2)(bmip)]$	0.1 mmol, 31 mg	0.15 mmol, 45 mg	0.25 mmol, 53 mg	EtOH	50%, 60 mg

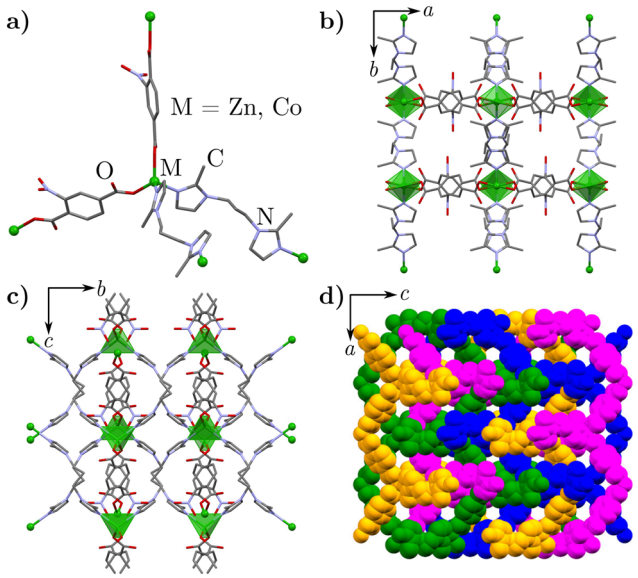

Fig. 2 Structure visualization of compounds **1** and **2**. a) Mononuclear building block {M(bdc-NO_2)$_2$(bmip)$_2$} (M = Zn, Co). Single framework views: b) along the *c*-axis; c) along the *a*-axis. d) 4-Fold interpenetration of frameworks. Hydrogen atoms and disordering are omitted for clarity.

921–922 (w), 875 (w), 824–839 (w), 773–778 (s), 721–724 (w), 691–693 (w), 580–581 (w), 508 (m), 440–445 (w).

3 Results and discussion

3.1 Synthesis, structure description, and characterization

All the compounds were obtained under similar reaction conditions. Metal nitrates were used as sources of metal ions, and the ratio of the metal ions, rigid carboxylate and flexible *N*,*N*′-ligand (bmip) was equimolar in all syntheses. The mixture of DMF and alcohol was used as a solvent. Cobalt compounds crystallize better in the DMF–methanol mixture, while zinc compounds are better formed in DMF–ethanol solutions. All syntheses were carried out at a temperature of 100 °C for 24 h. Compounds **1** and **2** were isolated as single crystals and they are isostructural. Single crystals of compound **3** were also obtained, but their quality was not enough for reliable determination of the crystal structure. In this regard, only a model of the structure with an *R*-factor of 13.4% was found.

According to single crystal X-ray data, the colorless crystals of [Zn(bdc-NO_2)(bmip)] (**1**) and purple crystals of [Co(bdc-NO_2)(bmip)] (**2**) are isostructural and crystallize in the orthorhombic space group *Ibca* (Fig. S1 and S4†). Asymmetric units in both structures contain one independent zinc(II) or cobalt(II) cation coordinated by the nitroterephthalate anion and a 1,3-bis(2-methylimidazolyl)propane moiety (Fig. S2 and S5†). Metal cations are in a distorted tetrahedral environment formed by two oxygen atoms of carboxyl groups and two nitrogen atoms of the bmip ligand. Arrangement of the bmip ligand around a two-fold axis results in two symmetry-related 2-methylimidazolyl rings and more complicated disordering of the propane moiety, which occupies 3 positions (Fig. S3†). The first position has occupancies of 0.383(21) and 0.214(16) in structures **1** and **2** correspondingly. The central carbon atom (C6) situates on a two-fold axis which results in two symmetry-related edged carbon atoms (C5). In the second and third positions the central carbon atom does not lie on the axis, which leads to two symmetry-related propane fragments with occupancies of 0.308(6) and 0.393(8) in structures **1** and **2** correspondingly. The nitro-terephthalate ring lies about an inversion centre so that the nitro-groups are disordered in two positions with half-occupancy. The metal–oxygen bond lengths are 1.949(3) Å and 1.960(4) Å and the metal–nitrogen bond lengths are 2.008(4) Å and 2.0234(7) Å for Zn and Co, respectively. Each metal atom connects two bmip ligands and two bdc-NO_2^{2-} anions (Fig. 2). Each bmip ligand as well as bdc-NO_2^{2-} anion is connected with two metal cations. Thus, metal atoms are interconnected *via* bridging bmip ligands and bdc-NO_2^{2-} anions to form a 4-fold interpenetrated densely packed metal–organic framework of diamond-like topology (***dia***).

Interestingly, pale-yellow crystals of [Zn(bdc-Br)(bmip)] (**3**), differing in composition from **1** only by the rigid carboxylate ligand, crystallize in the orthorhombic space group *Pccn* (Fig. S6†). According to the model of the structure of compound **3**, its atomic connectivity is quite similar to compound **1**. However, an asymmetric unit of compound **3** contains two Zn cations, two bromoterephthalate anions, and two bmip ligands. One of the bmip ligands is disordered by two equivalent positions. Zinc cations are in a distorted tetrahedral environment formed by two oxygen atoms of carboxylic groups and two nitrogen atoms of bmip ligands. The Zn–O bond lengths are in the range of 1.912(9)–1.971(9) Å, and the Zn–N bond lengths are in the range of 2.000(10)–2.020(10) Å. Zinc atoms are interconnected *via* organic ligands forming a 3D 4-fold interpenetrating framework with ***dia*** topology. Opposite to compound **1**, which is non-porous, compound **3** contains voids with sizes 3.5 × 3.5 Å. The overall void volume is 526 Å^3 per unit cell or 5.8% of cell volume. They are filled by disordered water molecules which is in good agreement with SQUEEZE calculations. According to calculations using Zeo++ software,[63] the voids are not accessible for exchange of guest molecules.

According to powder X-ray analysis, compound **4** is isostructural with compounds **2** and **1** based on nitroterephthalate, and not to **3** containing bdc-Br^{2-} anions (Fig. 3b). The reasons for the different crystal structure of compound **3** from both compounds **1** and **4** are not completely clear. The comparison of the SBU structures shows only slight changes in coordination angles in Zn coordination node and more pronounce differences in conformations of the flexible N-donor ligands (Fig. 4). However, such changes do not result in significant changes in coordination node geometry due to practically identical bmip ligand length and coordination angles. Nevertheless, it is sufficient to form quite different packing which is clearly seen from both the PXRD pattern and single crystal analysis (Fig. 3).

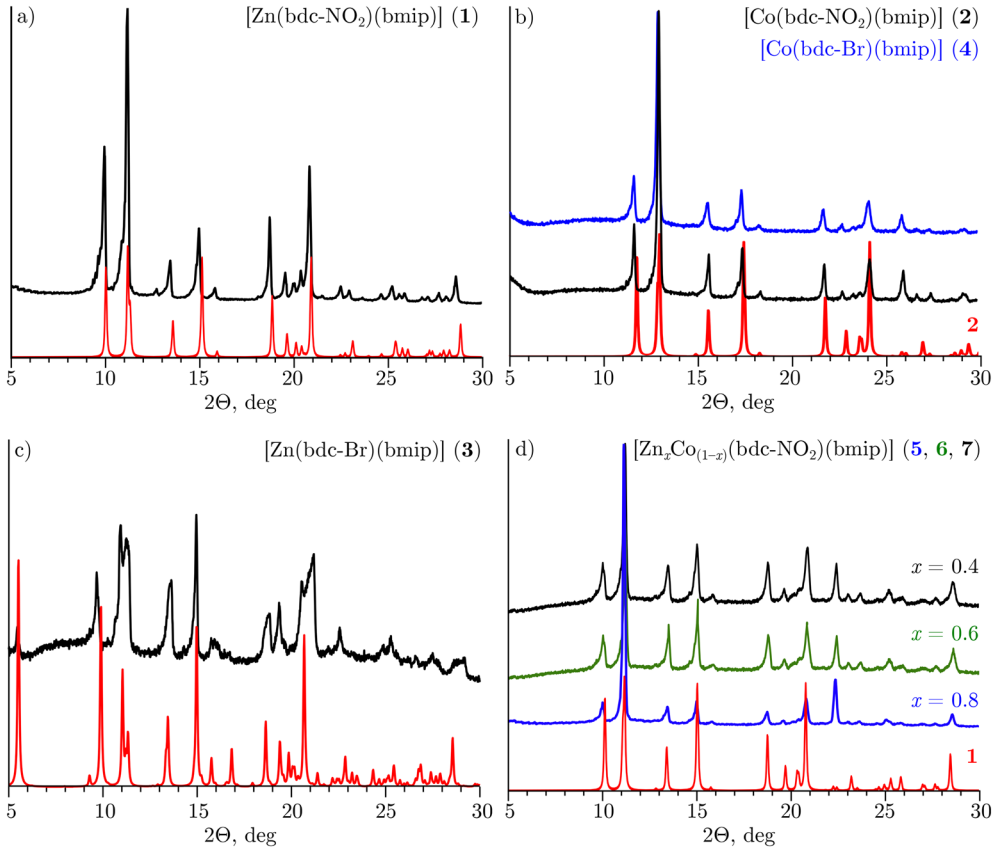

Fig. 3 Powder X-ray diffraction patterns for compounds: a) **1**; b) **2** and **4**; c) **3**; d) **5**–**7**. Red lines show simulated patterns for the corresponding compounds.

The isostructural nature of **1** and **2** makes it possible to obtain a series of solids with variable metal content. The ionic radii of Zn^{2+} (0.60 Å, 4-coordinate) and Co^{2+} (0.58 Å, 4-coordinate) are similar,[64] and thus replacement of Zn^{2+} ions by Co^{2+} is a viable route to afford mixed-metal compounds. Often, such substitution leads to materials with new properties.[51,65–67]

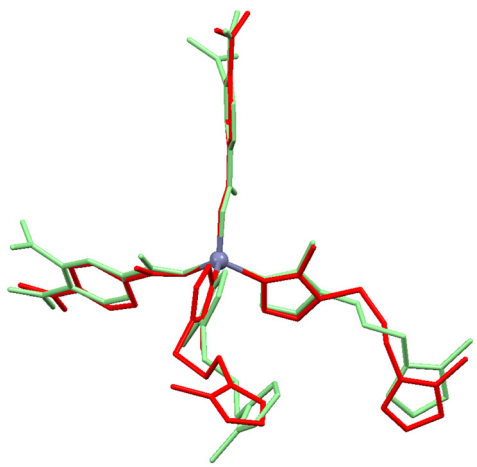

Fig. 4 Overlay of SBUs in **1** (light-green) and **3** (red). Hydrogen and bromine atoms are omitted and only one position of disordered fragments is shown for clarity.

To obtain such compounds, the method of pre-synthetic modification was chosen: a mixture of cobalt(II) and zinc(II) nitrates, as well as nitroterephthalic acid and bmip were used in syntheses in a given ratio. A series of mixed-metal phases $[Zn_xCo_{1-x}(bdc\text{-}NO_2)(bmip)]$ (x = 0.8(**5**), 0.6(**6**), 0.4(**7**)) were obtained as batches of small crystals. Visually, crystals in each batch are identical in colour and shape which indicates the formation of mixed-metal phases rather than separate Zn and Co phases. Single crystal X-ray analysis was not carried out for these crystals and their phase purity was established by powder X-ray analysis (Fig. 3d). The metal content in phases obtained was determined by atomic emission spectrometry which confirmed the composition specified by initial loadings to the synthetic mixture (see Table 1 and S1†).

It should be noted that often additional side groups, such as in our case methyl in imidazole moieties or nitro and bromo functional groups in rigid terephthalate linkers, can lead to the formation of non-interpenetrating structures due to steric hindrance of these substituents. In our previous work, it was shown that it is possible to change the interpenetration and porosity of cadmium MOFs during guest exchange.[41] However, all attempts to open up frameworks **1**–**7** using different liquid organic solvents were unsuccessful. All phases retain their dense 4-fold interpenetrated structures when kept in different organic solvents. All the compounds have no available pore volume

and therefore do not contain guest molecules. To our mind, the key factor for these differences is cation radii which affect the coordination mode (mono or bidentate) of carboxylate ligands and coordination angles. It is also likely that for Zn(II) it is more difficult to change the coordination angles required for transformation and structure opening due to its stronger Lewis acidity than Cd(II).

3.2 Luminescence properties

Transition metal complexes based on d^{10} metals have aroused enormous attention due to possible applications in the fields of sensing, light-emitting diodes and biological imaging.[6] Tuning the composition of compounds in a wide range opens possibilities for changing their optical properties. In our case, there are bromine or nitro-groups in the rigid carboxylate ligands which strongly differ by their electronic nature. Also, it is possible to vary metal content in the resulting compounds which should affect the luminescence behaviour. Taking into account this variability, we have measured the photoluminescence for all compounds obtained.

The luminescence of the free bmip ligand is characterized by the dependence of the emission wavelength on the excitation wavelength (Fig. S9†). The shift of the emission maxima is about 50 nm in the range of 510–560 nm when the excitation wavelength changes from 300 to 480 nm. The use of the bmip ligand in a dense interpenetrating MOF structure enhances this effect. The red shift of emission maxima in **1** reaches more than 100 nm in the range of 440–600 nm (Fig. S10†), which leads to change of emission color from blue to orange (Fig. S13†). Due to the d^{10} electron configuration of the Zn^{2+} cation, MLCT or LMCT processes are impossible. The observed emission of the coordination compound is attributed to $\pi^* \rightarrow \pi$ transition in the bmip ligand. The more pronounced red shift of luminescence maxima may be attributed to changes in the HOMO–LUMO energy levels of the bmip ligand upon coordination, which significantly increased the rigidity of the ligand.[41,42,68–70] The presence of nitro-groups in compound **1**, well-known quenching moieties, reduces significantly the quantum yield (QY) of this emission, which is less than 1%.

In contrast, zinc compound **3** without quenching moieties possesses bright photoluminescence (Fig. 5) with strong dependence of emission maxima wavelength on excitation wavelength. The red shift is slightly lower than that for compound **1** and is about 90 nm in the range of 460–550 nm with changing excitation wavelength from 360 to 500 nm, which results in changing of emission color from green-blue to yellow-orange (Fig. S14†). The luminescence of compound **3** excited at 420 nm is characterized by a relatively high QY of 39%.

Interestingly, the addition of Co(II) ions to compound **1** opens the possibility of a ligand-to-metal transition, and

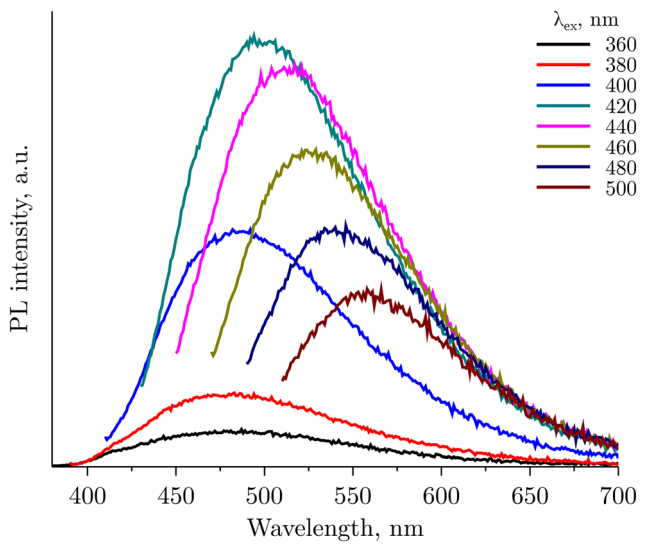

Fig. 5 Dependence of emission spectra of **3** on excitation wavelength.

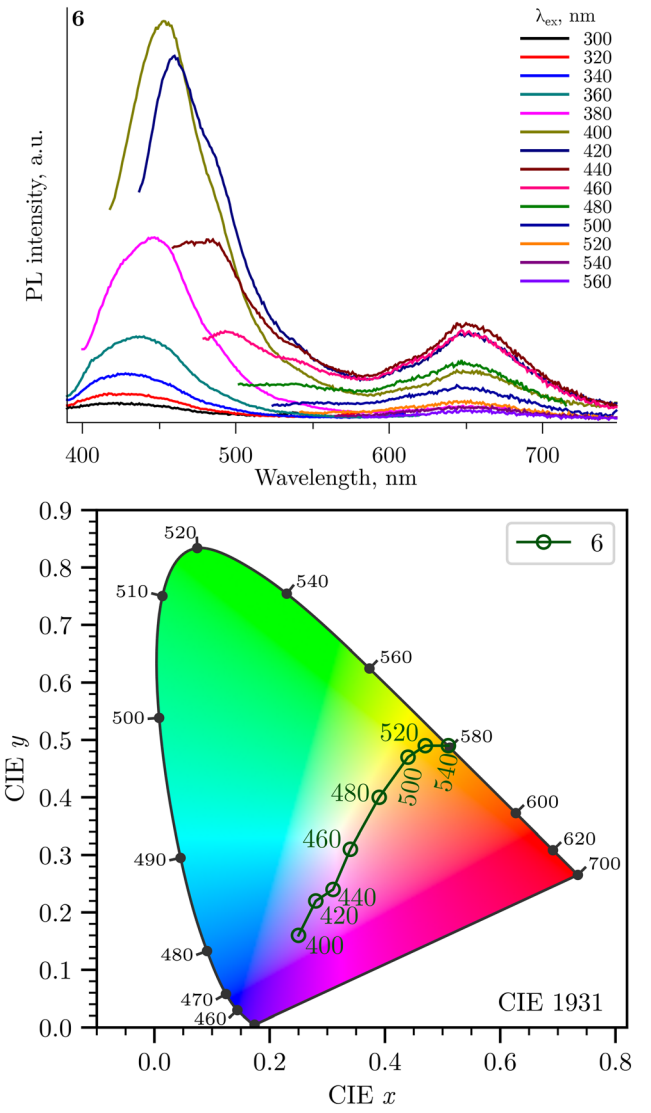

Fig. 6 Wavelength excitation dependence of the emission spectra and PL chromaticity for compound **6** at 300 K.

emission spectra of mixed-metal compounds **5**–**7** contain an additional band near 650 nm (Fig. 6, S11, and S12†). This emission band in the red region causes the emission colour to change from green to orange and further to red depending on the excitation wavelength (Fig. 6, S15, and S16†). For compound **6**, excitation at 460 nm results in almost white luminescence with color coordinates (0.34, 0.31) and color temperature of 5090 K which correspond to neutral white light.

4 Conclusions

As a result, a family of isostructural metal–organic coordination polymers of zinc(II) and cobalt(II) based on two types of ligands – structurally rigid terephthalates and structurally flexible 1,3-bis(2-methylimidazolyl)propane (bmip) – was obtained. Interestingly, Co(II) bmip-based MOFs with nitro- and bromoterephthalate are isostructural with Zn(II) nitroterephthalate, whereas the Zn-MOF with bromoterephthalate has another packing. Zn containing compounds demonstrate photoluminescence with strong dependence of emission maxima on excitation wavelength. The bathochromic shift for compounds **1** and **3** reaches 90–100 nm when the excitation wavelength changes from 300 to 480 nm. Compound **3** is characterized by a high quantum yield of 39%. The isostructural nature of **1** and **2** allow us to obtain mixed-metal phases **5**, **6**, and **7** with given metal ratios. Compounds **5**, **6**, and **7** reveal unusual luminescence behaviour. The addition of cobalt leads to the appearance of the second luminescence band in the red region and the shift of luminescence color from green to yellow, orange, and red. Compound **6** under 460 nm excitation demonstrates near white emission with CIE color coordinates of (0.34, 0.31).

We believe that a series of compounds with the general formula $[Zn_xCo_{1-x}(bdc\text{-}X)(bmip)]$ (x = 1, 0.8, 0.6, 0.4, 0; X = NO_2, Br) enhance the knowledge about MOFs based on two types of ligands: sterically rigid and flexible. Such a combination of ligands can lead both to flexible porous[41] or rigid compounds[42] due to multiple interpenetrations. The key factor affecting these results is cation radii.

Data availability

The data supporting this article have been included as part of the ESI.†

Author contributions

Pavel V. Burlak: investigation, writing – original draft. Denis G. Samsonenko: investigation, validation, writing – review & editing. Konstantin A. Kovalenko: conceptualization, validation, writing – original draft. Vladimir P. Fedin: validation, project administration, writing – review & editing.

Conflicts of interest

There are no conflicts to declare.

Acknowledgements

The authors are grateful to the Ministry of Science and Higher Education of the Russian Federation for financial support (Agreement No. 075-15-2022-263), providing an access to the large-scale research facility “EXAFS spectroscopy beamline”.

References

1 H. Huang, L. Wang, X. Zhang, H. Zhao and Y. Gu, *Clean Technologies*, 2023, **5**, 1–24.
2 K. A. Kovalenko, A. S. Potapov and V. P. Fedin, *Russ. Chem. Rev.*, 2022, **91**, RCR5026.
3 A. Luna-Triguero, J. M. Vicent-Luna, R. M. Madero-Castro, P. Gómez-Álvarez and S. Calero, *ACS Appl. Mater. Interfaces*, 2019, **11**, 31499–31507.
4 D. Britt, D. Tranchemontagne and O. M. Yaghi, *Proc. Natl. Acad. Sci. U. S. A.*, 2008, **105**, 11623–11627.
5 M. Ding, R. W. Flaig, H.-L. Jiang and O. M. Yaghi, *Chem. Soc. Rev.*, 2019, **48**, 2783–2828.
6 Y. Tang, H. Wu, W. Cao, Y. Cui and G. Qian, *Adv. Opt. Mater.*, 2021, **9**, 2001817.
7 X. Yu, A. A. Ryadun, D. I. Pavlov, T. Y. Guselnikova, A. S. Potapov and V. P. Fedin, *Angew. Chem., Int. Ed.*, 2023, **62**, e202306680.
8 X. Yu, A. A. Ryadun, A. S. Potapov and V. P. Fedin, *J. Hazard. Mater.*, 2023, **452**, 131289.
9 J. Geng, Y. Li, H. Lin, Q. Liu, J. Lu and X. Wang, *Dalton Trans.*, 2022, **51**, 11390–11396.
10 B. Fu, J. Chen, Y. Cao, H. Li, F. Gao, D.-Y. Guo, F. Wang and Q. Pan, *Sens. Actuators, B*, 2022, **369**, 132261.
11 W. Dong, Y.-Q. Sun, B. Yu, H.-B. Zhou, H.-B. Song, Z.-Q. Liu, Q.-M. Wang, D.-Z. Liao, Z.-H. Jiang, S.-P. Yan and P. Cheng, *New J. Chem.*, 2004, **28**, 1347.
12 D. Sun, S. Yuan, H. Wang, H.-F. Lu, S.-Y. Feng and D.-F. Sun, *Chem. Commun.*, 2013, **49**, 6152.
13 S. Yuan, Y.-K. Deng and D. Sun, *Chem. – Eur. J.*, 2014, **20**, 10093–10098.
14 R. Haldar, S. Bhattacharyya and T. K. Maji, *J. Chem. Sci.*, 2020, **132**, 99.
15 D. N. Dybtsev and K. P. Bryliakov, *Coord. Chem. Rev.*, 2021, **437**, 213845.
16 Z. Wu, Y. Li, C. Zhang, X. Huang, B. Peng and G. Wang, *Chem Catal.*, 2022, **2**, 1009–1045.
17 S. Li, J. Sun, G. Liu, S. Zhang, Z. Zhang and X. Wang, *Chin. Chem. Lett.*, 2024, **35**, 109148.
18 Y. Liu, W. Xuan and Y. Cui, *Adv. Mater.*, 2010, **22**, 4112–4135.
19 M. Viciano-Chumillas, M. Mon, J. Ferrando-Soria, A. Corma, A. Leyva-Pérez, D. Armentano and E. Pardo, *Acc. Chem. Res.*, 2020, **53**, 520–531.
20 K. Jin, B. Lee and J. Park, *Coord. Chem. Rev.*, 2021, **427**, 213473.
21 R. Medishetty, J. K. Zaręba, D. Mayer, M. Samoć and R. A. Fischer, *Chem. Soc. Rev.*, 2017, **46**, 4976–5004.
22 B. Mohan, S. Kumar, H. Xi, S. Ma, Z. Tao, T. Xing, H. You, Y. Zhang and P. Ren, *Biosens. Bioelectron.*, 2022, **197**, 113738.

23 G. Dzhardimalieva, V. Zhinzhilo and I. Uflyand, *Russ. Chem. Rev.*, 2022, **91**, 5055.
24 P. V. Alekseevskiy, S. Rzhevskiy, V. Gilemkhanova, N. K. Kulachenkov, A. Sapianik, M. Barsukova, V. P. Fedin and V. A. Milichko, *Adv. Mater. Interfaces*, 2021, **8**, 2170131.
25 M. I. Rogovoy, T. S. Frolova, D. G. Samsonenko, A. S. Berezin, I. Y. Bagryanskaya, N. A. Nedolya, O. A. Tarasova, V. P. Fedin and A. V. Artem'ev, *Eur. J. Inorg. Chem.*, 2020, **2020**, 1635–1644.
26 S. Bhattacharjee, C. Chen and W.-S. Ahn, *RSC Adv.*, 2014, **4**, 52500–52525.
27 J. H. Cavka, S. Jakobsen, U. Olsbye, N. Guillou, C. Lamberti, S. Bordiga and K. P. Lillerud, *J. Am. Chem. Soc.*, 2008, **130**, 13850–13851.
28 S. S.-Y. Chui, S. M.-F. Lo, J. P. H. Charmant, A. G. Orpen and I. D. Williams, *Science*, 1999, **283**, 1148–1150.
29 S. A. Sapchenko, D. N. Dybtsev, D. G. Samsonenko, R. V. Belosludov, V. R. Belosludov, Y. Kawazoe, M. Schröder and V. P. Fedin, *Chem. Commun.*, 2015, **51**, 13918–13921.
30 D. N. Dybtsev, H. Chun and K. Kim, *Angew. Chem., Int. Ed.*, 2004, **43**, 5033–5036.
31 D. Sun, Z.-H. Yan, V. A. Blatov, L. Wang and D.-F. Sun, *Cryst. Growth Des.*, 2013, **13**, 1277–1289.
32 D. Sun, Z.-H. Yan, Y.-K. Deng, S. Yuan, L. Wang and D.-F. Sun, *CrystEngComm*, 2012, **14**, 7856.
33 Z.-J. Lin, J. Lü, M. Hong and R. Cao, *Chem. Soc. Rev.*, 2014, **43**, 5867–5895.
34 A. Schneemann, V. Bon, I. Schwedler, I. Senkovska, S. Kaskel and R. A. Fischer, *Chem. Soc. Rev.*, 2014, **43**, 6062–6096.
35 C. Pettinari, A. Tăbăcaru and S. Galli, *Coord. Chem. Rev.*, 2016, **307**, 1–31.
36 R. E. Morris and L. Brammer, *Chem. Soc. Rev.*, 2017, **46**, 5444–5462.
37 J. Wang, L. Lu, J.-R. He, W.-P. Wu, C. Gong, L. Fang, Y. Pan, A. K. Singh and A. Kumar, *J. Mol. Struct.*, 2019, **1182**, 79–86.
38 X.-P. Wang, W.-M. Chen, H. Qi, X.-Y. Li, C. Rajnák, Z.-Y. Feng, M. Kurmoo, R. Boča, C.-J. Jia, C.-H. Tung and D. Sun, *Chem. – Eur. J.*, 2017, **23**, 7990–7996.
39 M. O. Barsukova, D. G. Samsonenko, T. V. Goncharova, A. S. Potapov, S. A. Sapchenko, D. N. Dybtsev and V. P. Fedin, *Russ. Chem. Bull.*, 2016, **65**, 2914–2919.
40 M. O. Barsukova, S. A. Sapchenko, K. A. Kovalenko, D. G. Samsonenko, A. S. Potapov, D. N. Dybtsev and V. P. Fedin, *New J. Chem.*, 2018, **42**, 6408–6415.
41 P. V. Burlak, D. G. Samsonenko, K. A. Kovalenko and V. P. Fedin, *Inorg. Chem.*, 2023, **62**, 18087–18097.
42 P. V. Burlak, D. G. Samsonenko, K. A. Kovalenko and V. P. Fedin, *Polyhedron*, 2022, **222**, 115880.
43 Y. Wei, B. Zhu, J. Wang, L. Wang, R. Wu, W. Liu, B. Ma, D. Yang, Y. Fan and X. Zhang, *CrystEngComm*, 2021, **23**, 6376–6387.
44 H. Xu, B.-Y. Zhou, K. Yu, Z.-H. Su, B.-B. Zhou and Z.-M. Su, *CrystEngComm*, 2019, **21**, 1242–1249.
45 D.-S. Zhang, Y.-Z. Zhang, J. Gao, H.-L. Liu, H. Hu, L.-L. Geng, X. Zhang and Y.-W. Li, *Dalton Trans.*, 2018, **47**, 14025–14032.
46 G.-L. Wen, W.-P. Wu, F.-W. Wang, D.-F. Liu, X.-L. Wang, J.-W. Rong and Y.-Y. Wang, *CrystEngComm*, 2021, **23**, 6171–6179.
47 R. Wu, C. Bi, L. Wang, J. Wang, C. Fan, N. Li, M. Wang, F. Shao, G. Chen and Y. Fan, *Synth. Met.*, 2021, **277**, 116786.
48 Y. Yang, C. Tu, Z. Liu, J. Wang, X. Yang and F. Cheng, *Polyhedron*, 2021, **206**, 115339.
49 A. D. Burrows, *CrystEngComm*, 2011, **13**, 3623.
50 X. Yang and Q. Xu, *Cryst. Growth Des.*, 2017, **17**, 1450–1455.
51 A. Nqombolo, T. S. Munonde, T. A. Makhetha, R. M. Moutloali and P. N. Nomngongo, *J. Mater. Res. Technol.*, 2021, **12**, 1845–1855.
52 Z. Gu, X. Wei, X. Zhang, Z. Duan, Z. Gu, Q. Gong and K. Luo, *Small*, 2021, **17**, 2104125.
53 R. Jaryal, R. Kumar and S. Khullar, *Coord. Chem. Rev.*, 2022, **464**, 214542.
54 Q. Hao, X. Qian, L. Jin, J. Cheng, S. Zhao, J. Chen, K. Zhang, B. Li, S. Pang and X. Shen, *J. Alloys Compd.*, 2023, **967**, 171605.
55 M. Y. Masoomi, A. Morsali, A. Dhakshinamoorthy and H. Garcia, *Angew. Chem., Int. Ed.*, 2019, **58**, 15188–15205.
56 L. Feng, K.-Y. Wang, G. S. Day and H.-C. Zhou, *Chem. Soc. Rev.*, 2019, **48**, 4823–4853.
57 L. Chen, H.-F. Wang, C. Li and Q. Xu, *Chem. Sci.*, 2020, **11**, 5369–5403.
58 V. A. Blatov, A. P. Shevchenko and D. M. Proserpio, *Cryst. Growth Des.*, 2014, **14**, 3576–3586.
59 M. O'Keeffe, M. A. Peskov, S. J. Ramsden and O. M. Yaghi, *Acc. Chem. Res.*, 2008, **41**, 1782–1789.
60 E. V. Alexandrov, V. A. Blatov, A. V. Kochetkov and D. M. Proserpio, *CrystEngComm*, 2011, **13**, 3947–3958.
61 A. P. Shevchenko and V. A. Blatov, *Struct. Chem.*, 2021, **32**, 507–519.
62 E. V. Alexandrov, A. P. Shevchenko and V. A. Blatov, *Cryst. Growth Des.*, 2019, **19**, 2604–2614.
63 T. F. Willems, C. H. Rycroft, M. Kazi, J. C. Meza and M. Haranczyk, *Microporous Mesoporous Mater.*, 2012, **149**, 134–141.
64 R. D. Shannon, *Acta Crystallogr., Sect. A: Cryst. Phys., Diffr., Theor. Gen. Crystallogr.*, 1976, **32**, 751–767.
65 V. V. Butova, V. A. Polyakov, A. P. Budnyk, A. M. Aboraia, E. A. Bulanova, A. A. Guda, E. A. Reshetnikova, Y. S. Podkovyrina, C. Lamberti and A. V. Soldatov, *Polyhedron*, 2018, **154**, 457–464.
66 S. Abednatanzi, P. G. Derakhshandeh, H. Depauw, F.-X. Coudert, H. Vrielinck, P. V. D. Voort and K. Leus, *Chem. Soc. Rev.*, 2019, **48**, 2535–2565.
67 M. Y. Masoomi, A. Morsali, A. Dhakshinamoorthy and H. Garcia, *Angew. Chem., Int. Ed.*, 2019, **58**, 15188–15205.
68 M. Arıcı, Y. C. Dikilitaş, H. Erer and O. Z. Yeşilel, *CrystEngComm*, 2020, **22**, 5776–5785.
69 R. Singh and P. K. Bharadwaj, *Cryst. Growth Des.*, 2013, **13**, 3722–3733.
70 J.-F. Lu and Z.-H. Liu, *J. Coord. Chem.*, 2016, **69**, 2553–2562.